1862 *Biochemistry* **2010,** *49,* 1862–1872
DOI: 10.1021/bi901848m

BIOCHEMISTRY
including biophysical chemistry & molecular biology
Article

Refolding and Characterization of a Soluble Ectodomain Complex of the Calcitonin Gene-Related Peptide Receptor

Christopher M. Koth,[‡,∥] Norzehan Abdul-Manan,[‡] Christopher A. Lepre,[‡] Peter J. Connolly,[‡] Sanghee Yoo,[§] Arun K. Mohanty,[‡] Judith A. Lippke,[‡] Jacque Zwahlen,[‡] Joyce T. Coll,[‡] John D. Doran,[‡] Miguel Garcia-Guzman,[§] and Jonathan M. Moore*[,‡]

[‡]*Vertex Pharmaceuticals Inc., 130 Waverly Street, Cambridge, Massachusetts 02139, and* [§]*Vertex Pharmaceuticals San Diego LLC, 11010 Torreyana Road, San Diego, California 92121.* [∥]*Present address: Genentech, Inc., 1 DNA Way, MS 27, South San Francisco, CA 94080.*

Received October 28, 2009; Revised Manuscript Received January 22, 2010

ABSTRACT: The calcitonin gene-related peptide (CGRP) receptor is a heterodimer of two membrane proteins: calcitonin receptor-like receptor (CLR) and receptor activity-modifying protein 1 (RAMP1). CLR is a class B G-protein-coupled receptor (GPCR), possessing a characteristic large amino-terminal extracellular domain (ECD) important for ligand recognition and binding. Dimerization of CLR with RAMP1 provides specificity for CGRP versus related agonists. Here we report the expression, purification, and refolding of a soluble form of the CGRP receptor comprising a heterodimer of the CLR and RAMP1 ECDs. The extracellular protein domains corresponding to residues 23−133 of CLR and residues 26−117 of RAMP1 were shown to be sufficient for formation of a stable, monodisperse complex. The binding affinity of the purified ECD complex for the CGRP peptide was significantly lower than that of the native receptor (IC_{50} of 12 μM for the purified ECD complex vs 233 pM for membrane-bound CGRP receptor), indicating that other regions of CLR and/or RAMP1 are important for peptide agonist binding. However, high-affinity binding to known potent and specific nonpeptide antagonists of the CGRP receptor, including olcegepant and telcagepant ($K_D < 0.02\,\mu$M), as well as N-terminally truncated peptides and peptide analogues (140 nM to 1.62 μM) was observed.

The 37-amino acid calcitonin gene-related peptide (CGRP)[1] is the most potent endogenous vasodilator known (*1*). In the brain, it is released from cell bodies in the trigeminal ganglia, where it functions locally with its receptors to cause dilation of cerebral blood vessels. Enhanced release of CGRP exacerbates cranial vasodilation and is thought to be a primary determinant in the pathogenesis of migraine headaches (*2*, *3*). Several key observations support the role of CGRP in migraine. For example, early studies detected CGRP at elevated levels in jugular venous blood, but not in peripheral blood (*4*), and intravenous administration of CGRP rapidly induced headache and other migraine-like disorders in migraine-susceptible patients (*5*). The strongest evidence, however, comes from recent clinical trials in which the potent and selective CGRP receptor antagonists olcegepant (BIBN4096BS) (*6*) and telcagepant (MK-0974) (*7*) were efficacious in treatment of acute migraine.

*To whom correspondence should be addressed: Vertex Pharmaceuticals Inc., 130 Waverly St., Cambridge, MA 02139. E-mail: Jonathan_Moore@vrtx.com. Phone: (617) 444-6444. Fax: (617) 444-6688.

[1]Abbreviations: BSA, bovine serum albumin; CGRP, calcitonin gene-related peptide; CRFR2, corticotropin releasing factor type 2; CLR, calcitonin receptor-like receptor; DMSO, dimethyl sulfoxide; DTT, dithiothreitol; ECD, extracellular domain; EDTA, ethylenediaminetetraacetic acid; GPCR, G-protein-coupled receptor; HEPES, 4-(2-hydroxyethyl)-1-piperazineethanesulfonic acid; NMR, nuclear magnetic resonance; NOE, nuclear Overhauser enhancement; PEI, polyethyleneimine; P20, polyoxyethylene-20-sorbitan monolaurate; RAMP, receptor activity-modifying protein; SPR, surface plasmon resonance; TRIS, tris(hydroxymethyl)aminomethane; TROSY, transverse relaxation-optimized spectroscopy.

The receptor for CGRP is a heterodimer of the calcitonin receptor-like receptor (CLR) and receptor activity-modifying protein 1 (RAMP1). CLR is a member of the class B (type II) G-protein-coupled receptor (GPCR) family that includes receptors for parathyroid hormone, glucagon, secretin, gastric inhibitory peptide, and corticotropin releasing factor. RAMPs are accessory membrane proteins required for the proper subcellular localization, function, and selectivity of certain class B GPCRs (*8*). When expressed alone, CLR is not known to bind any ligand (*9*). However, when coexpressed with RAMP1, it functions as a cell surface receptor for CGRP and has moderate affinity for adrenomedullin (*8*). CLR is also capable of heterodimerizing with two other RAMP proteins (RAMP2 and RAMP3), which generates receptors with selectivity for adrenomedullin (reviewed in ref *10*).

Several classes of CGRP receptor antagonists have been identified. The first peptide antagonists were simply N-terminal truncations of the CGRP peptide (*11*−*14*). Later, more potent peptide antagonists included non-natural C-terminal fragments of CGRP (*15*, *16*). The prototype nonpeptide antagonist, olcegepant (Figure 1, compound **1**), was discovered through cellular-based screens and subsequent chemical optimization. Olcegepant is a selective antagonist of the human CGRP receptor (K_i = 0.014 nM) (*17*). Although the compound displays poor oral bioavailability, early clinical trials provided proof of concept linking CGRP receptor antagonism with successful treatment of migraine (*18*). More recently, the first orally bioavailable CGRP receptor antagonist, telcagepant (also known as MK-0974), has shown efficacy in migraine treatment (*7*).

 Published on Web 01/25/2010

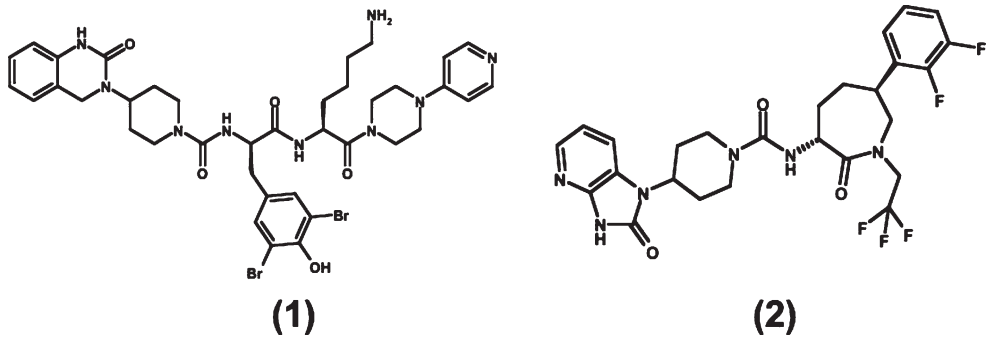

FIGURE 1: Chemical structures of olcegepant (compound **1**) and telcagepant (compound **2**).

The extracellular domains (ECDs) of CLR and RAMP1 have been shown to play essential roles in heterodimerization and membrane trafficking, agonist binding and selectivity, and antagonist recognition. For example, using deletion mutants and chimeric constructs of CLR (*19*) and RAMP1 (*20*), regions were identified in the ECDs of both proteins that are essential for receptor dimerization and trafficking. Similar mutational approaches implicate the N-terminal sequences of RAMP1 (*21*, *22*) and CLR (*23*) in conferring agonist binding specificity.

Several studies have also identified the N-terminal domains as being important determinants for antagonist binding. For example, key residues in CLR (localized to amino acids 37−63) were shown to confer high-affinity antagonist binding for an iodinated analogue of olcegepant (*24*). More importantly, selectivity of olcegepant for the CGRP receptor versus related receptors appears to be due to a specific interaction with the extracellular region of RAMP1. Moreover, [^{125}I]CGRP cross-linking studies indicate that the CLR and RAMP1 ECDs are situated close to the CGRP binding site, suggesting that both protein domains together define the antagonist binding pocket (*22*).

As with most GPCRs, biochemical, biophysical, and structural studies of the CGRP receptor have been hindered by its membrane localization and the lack of an abundant natural source for purification. Furthermore, the dimeric nature of the receptor and the presence of several disulfide bonds in both CLR and RAMP1 exacerbate the challenges of recombinant production beyond those of the monomeric class B GPCR ectodomains (*25*, *26*). In this study, we present a reductionist approach for the production of the CGRP receptor that focuses on the soluble ECDs of CLR and RAMP1. We have identified, purified, and characterized a soluble core complex that serves as a valid surrogate for studying binding of a small-molecule antagonist to the CGRP receptor. To the best of our knowledge, this study also represents the first isolation of any class B GPCR−RAMP complex that is amenable to high-resolution structural studies (E. ter Haar, C. K. Koth, N. Abdul-Manan, L. Swenson, J. Coll, J. A. Lippke, C. A. Lepre, M. Garcia-Guzman, and J. M. Moore, unpublished observations). Our results contribute further insight into the structure and function of the CGRP receptor and identify a complex suitable for structural analysis by nuclear magnetic resonance (NMR) spectroscopy and X-ray crystallography.

EXPERIMENTAL PROCEDURES

Materials. cDNA clones for human CLR (AY389506) and human RAMP1 (AY265457) were purchased from the Missouri S&T cDNA Resource Center. *Pfu* DNA polymerase was from Stratagene (La Jolla, CA), and KlenTaq was purchased from Ab Peptides (St. Louis, MO). The pET28b vector and BL21(DE3) Rosetta 2 cells were purchased from Novagen (Milwaukee, WI). $^{15}NH_4Cl$, [^{13}C]glucose, D_2O, and additional isotopes for generating methyl-protonated samples (*27*) were purchased from Cambridge Isotope Laboratories (Andover, MA). The MONO Q HR 10/10 and S200 26/60 gel filtration columns and Vivaspin concentrators were purchased from GE Healthcare (Piscataway, NJ), as were [^{125}I]CGRP and Biacore reagents and chips. An UNO Q-6 column was purchased from Bio-Rad (Hercules, CA). SK-N-MC membranes were from Perkin-Elmer (Waltham, MA). The CGRP peptide and truncated variants were obtained from American Peptide (Sunnyvale, CA). Olcegepant and telcagepant were synthesized in house using previously published methods (*28*, *29*). Amine-PEG2-biotin was from Pierce (Rockford, IL). Five millimeter microcell NMR tubes were from Shigemi, Inc. (Alison Park, PA).

Construct Cloning and Expression. Truncations of CLR were PCR amplified from the parent cDNA using cloned *Pfu* DNA Polymerase and KlenTaq, with the NcoI and XhoI restriction sites incorporated into the PCR primers for subsequent subcloning into pET28b. A stop codon was incorporated at the 3′ end of CLR constructs, for expression without a fusion tag. Truncations of RAMP1 were PCR amplified as described above, using the NdeI and XhoI restriction sites for subcloning into pET28b, downstream of the coding sequence for a hexahistidine tag and thrombin cleavage site.

Escherichia coli BL21(DE3) Rosetta 2 cells were transformed with the plasmids described above and were grown at 37 °C and 225 rpm to an OD_{600} of 0.4−0.6 and then induced with 0.5 mM isopropyl 6-D-thiogalactopyranoside (IPTG). The cells were grown for an additional 3 h at 37 °C before being harvested. For isotopically labeled proteins, M9 minimal medium containing $^{15}NH_4Cl$, [^{13}C]glucose, and/or D_2O was used. Methyl-protonated {Ile(δ1 only),Leu($^{13}CH_3$,$^{12}CD_3$),Val($^{13}CH_3$,$^{12}CD_3$)} samples were prepared as described previously (*27*). For CLR, a shorter construct lacking seven amino-terminal residues (CLR_{30-133}) had a higher level of expression in minimal medium (data not shown) and was used for all perdeuterated samples.

Luria broth was used for unlabeled proteins. Cell pellets (typically 0.7 g/L from M9 medium and 1.2 g/L from Luria broth) were flash-frozen in liquid nitrogen and stored at −70 °C.

Inclusion Body Preparation of CLR and RAMP1. Inclusion body and refolding procedures are based on those previously reported by Chauhan et al. for the isolated CLR ECD (*25*). Several modifications were made to yield a CLR_{23-133}−$RAMP1_{26-117}$ ECD complex, as detailed below. Briefly, 12−15 g of frozen cells (for either CLR_{23-133} or $RAMP1_{26-117}$) was resuspended in

100 mL of buffer A [100 mM Tris-HCl and 1 mM EDTA (pH 7.0)] and lysed with a microfluidizer using one pass at 15000 psi. Lysed cells were mixed with 50 mL of buffer B [100 mM Tris-HCl, 150 mM NaCl, and 1.5% Triton X-100 (pH 7.0)] and pelleted by centrifugation at 50000*g* for 30 min. The inclusion body pellet was washed twice in 35 mL of buffer C [100 mM Tris-HCl, 150 mM NaCl (pH 7.0), and 0.5% Triton X-100] followed by two additional 35 mL buffer washes without Triton X-100. Each wash cycle was followed by centrifugation at 30000*g* for 15 min and resuspension of the pellet in wash buffer. The washed inclusion body pellet was then solubilized in 35 mL of buffer D [6 M guanidine hydrochloride, 100 mM DTT, 100 mM Tris (pH 8.0), and 5 mM EDTA] by being stirred at room temperature for 1−2 h, followed by centrifugation at 50000*g* for 30 min. Removal of DTT was achieved by dialysis with 2 L of buffer E [4 M guanidine hydrochloride and 100 mM sodium phosphate (pH 6.0)] for 12−16 h, followed by two additional fresh buffer changes. The dialyzed, denatured protein was centrifuged at 50000*g* for 30 min, quantitated (using absorbance at 280 nm), and frozen at −70 °C until it was needed.

Protein Refolding and Purification. The ECD CLR_{23-133}−$RAMP1_{26-117}$ complex was prepared by co-refolding of the ECD proteins from inclusion bodies generated using the procedure described above. Equimolar amounts of CLR_{23-133} and $RAMP1_{26-117}$ inclusion body preparations were mixed and diluted to 100 mL in buffer E to a final protein concentration of 0.1−0.2 mg/mL, followed by dialysis at 4 °C for 24 h against 2 L of refolding buffer F [1 M L-arginine, 1 mM EDTA, 0.05 M sodium phosphate (pH 8.0), and 5 mM reduced glutathione and 1 mM oxidized glutathione, respectively]. The protein was then further dialyzed against 2 L of buffer G [20 mM Tris-HCl, 1 mM EDTA, 10% glycerol, and 50 mM NaCl (pH 7.3)] for 12 h at 4 °C, followed by a change to fresh buffer G and dialysis for an additional 12 h, also at 4 °C. The precipitated protein was removed by centrifugation at 30000*g* for 30 min. After filtration through a 0.2 μm filter, the refolded CLR_{23-133}−$RAMP1_{26-117}$ complex was applied to an anion-exchange MONO Q HR 10/10 or UNO Q-6 column at 1.5 mL/min and resolved using a linear sodium chloride gradient from 50 to 600 mM in buffer G. Fractions were analyzed by SDS−PAGE, and those containing the co-eluted CLR_{23-133}−$RAMP1_{26-117}$ complex were pooled and concentrated (Vivaspin molecular mass cutoff of 10 kDa) to 2 mg/mL followed by thrombin cleavage at 4 °C overnight to remove the hexahistidine on $RAMP1_{26-117}$ (1 unit of thrombin/2 mg of purified CLR_{23-133}−$RAMP1_{26-117}$ complex). Cleaved protein was applied to an S200 26/60 gel filtration column at a flow rate of 1.0 mL/min in buffer H [20 mM Tris-HCl, 150 mM NaCl, 1 mM EDTA, and 10% glycerol (pH 7.3)]. Fractions containing the co-eluted CLR_{23-133}−$RAMP1_{26-117}$ ECD complex were pooled and concentrated to 10−20 mg/mL. Purified proteins were used immediately in functional or structural studies or flash-frozen in liquid nitrogen and stored at −70 °C until they were needed.

[^{125}I]CGRP Binding Displacement Assay. The SK-N-MC neuroblastoma cell line expresses well-characterized CGRP receptor activity (*30*). SK-N-MC membranes (12 μg) were incubated with a competing ligand (CGRP, olcegepant, or purified CLR_{23-133}−$RAMP1_{26-117}$ ECD complex) for 10 min prior to addition of 46 pM [^{125}I]CGRP. After incubation for 2 h at room temperature, the reaction was stopped by rapid filtration through a GF/C filter plate (Perkin-Elmer, Waltham, MA) pretreated with 0.5% PEI and 0.5% BSA. The filter plate was washed with ice-cold wash buffer [50 mM Tris-HCl (pH 7.4), 5 mM $MgCl_2$, and 0.1% BSA] using a cell harvester (Tomtec, Hamden, CT). The radioactivity of the filter plates, corresponding to bound [^{125}I]CGRP, was read on a Topcount plate reader (Packard Instrument Co., Meriden, CT). Nonspecific binding was assessed in the presence of 1 μM olcegepant. IC_{50} values were calculated by nonlinear regression using Prism 5 (GraphPad Software, La Jolla, CA).

CLR_{23-133}−$RAMP1_{26-117}$ Competition Assay. Increasing concentrations of CGRP or the small-molecule antagonist olcegepant were incubated with 1 μM CLR_{23-133}−$RAMP1_{26-117}$ complex for 15−20 min at room temperature. After this incubation, 12 μg of SK-N-MC membranes was added, followed by 46 pM [^{125}I]CGRP. These mixtures were then incubated for 2 h, and the amount of [^{125}I]CGRP remaining bound to wild-type CGRP receptors in the SK-N-MC membranes was measured, as described above.

Steady State Fluorescence Spectroscopy. Fluorescence measurements were performed in a Perkin-Elmer LS50B luminescent spectrometer. One milliliter of a 4 μM solution of the CLR_{23-133}−$RAMP1_{26-117}$ complex in 10 mM Tris, 125 mM NaCl, and 1 mM EDTA (pH 7.3) was kept in the cuvette compartment with stirring at room temperature. Fluorescence emission spectra exhibiting trytophan quenching were recorded at 0, 1, 2, 3, and 4 μM olcegepant. This was accomplished via addition of successive 1 μL aliquots of a 10 mM olcegepant stock solution in DMSO to the cuvette. A λ_{ex} of 290 nm was used, and an emission range from 300 to 400 nm. The final absorbance of a 4 μM solution of olcegepant at 290 nm is less than 0.1 absorbance unit; hence, there was no need to correct for inner filter effects.

Surface Plasmon Resonance. SPR data were collected on a Biacore 3000 instrument (GE Healthcare) at 25 °C. We conducted competition binding experiments by monitoring the response from immobilized CGRP upon titration of the CLR_{23-133}−$RAMP1_{26-117}$ ECD complex premixed with different concentrations of compounds or peptides. The assay buffer was HBS-P [10 mM HEPES, 150 mM NaCl, and 0.005% P20 (pH 7.5)] with or without 2% DMSO, as indicated. N-Terminally biotinylated, 37-residue CGRP was dialyzed against HBS-P buffer prior to immobilization on a Biacore streptavidin sensor chip (SA chip) following standard protocols provided by the manufacturer (Biacore 3000 Instrument Handbook, January 2001 Edition). Biotinylated CGRP was immobilized on flow cell 2, yielding 1500−2000 response units. Flow cell 1 was used as a reference cell. Both flow cell surfaces were blocked with two 6 min injections of 0.5 mM amine-PEG2-biotin at a flow rate of 10 μL/min.

The protein concentration was determined using an extinction coefficient of 62170 M^{-1} cm^{-1} at 280 nm. A competition ligand binding assay was conducted with the compounds telcagepant and olcegepant and full-length and truncated CGRP peptides (Table 2). The ECD CLR_{23-133}−$RAMP1_{26-117}$ complex (0.2 or 0.8 μM) was mixed with different amounts of compounds and peptides and incubated for 30 min at room temperature before being injected onto the SA chip containing immobilized 37-residue CGRP. For titrations of mixtures containing compounds, all buffers were supplemented with 2% DMSO. Each protein/compound mixture was injected to the surface for 90 s at a flow rate of 50 μL/min followed by a 5 min delay to allow for protein dissociation. Surfaces were regenerated with 20 s injections of 10 mM glycine at pH 3.0.

The SPR data were evaluated using BIAevaluation version 3.1 (GE Healthcare) and Prism 5 (GraphPad Software). The surface

Table 1: Summary of Deletion Constructs for CLR and RAMP1 Used To Prepare 1:1 Complexes for Crystal Trials[a]

CLR	RAMP1
E23−E133	A26−S117
E23−E133	A26−D113
E23−E133	A26−R109
E23−E133	A26−P105
D30−E133	A26−S117
D30−E133	A26−D113
D30−E133	A26−R109
D30−E133	A26−P105
G35−T131	A26−S117
G35−T131	A26−D113
G35−T131	A26−R109
G35−T131	A26−P105
K40−E133	A26−S117
K40−E133	A26−D113
K40−E133	A26−P109
K40−E133	A26−P105

[a]The complex of CLR_{23-133} and $RAMP1_{26-117}$ formed diffracting crystals.

responses at each compound or peptide concentration were obtained from BIAevaluation, and the data were fit by Prism using the equation

$$Y = P_1(A_0 - 0.5\{[A_0 + X + K_d] - [(A_0 + X + K_d)(A_0 + X + K_d) - 4A_0X]^{1/2}\})$$

where A_0 is the protein concentration, K_d is the constant for dissociation of the compound from the protein, P_1 is a constant, which is dependent on the active ligand concentration on the surface and its dissociation constant for dissociation from the ectodomain protein, X is the compound concentration, and Y is the resonance response.

NMR Spectroscopy. NMR resonance assignment and ligand binding studies of the unlabeled CLR_{23-133}−[^{15}N,^{13}C,^{2}H]$RAMP1_{26-117}$ complex were conducted in a 5 mm microcell NMR tube containing 300 μL of 300 μM protein in 50 mM Tris (pH 7.3), 50 mM NaCl, and 5% D_2O. Ligands were added in small aliquots of a concentrated [^{2}H]DMSO stock solution to a final molar excess of 1.2-fold. The final [^{2}H]DMSO concentration in the samples was < 5%, and a [^{2}H]DMSO-only control was run to account for solvent-induced perturbations. All NMR experiments were conducted at 303 K on a Bruker Avance 800 MHz spectrometer equipped with an inverse triple-resonance (TXI), Z-axis gradient cryprobe. ^{15}N−^{1}H TROSY spectra were recorded using published methods (*31*). Three-dimensional triple-resonance data were acquired using methods similar to those described previously (*32*, *33*). Data were processed using either TopSpin 1.3 (Bruker-Spectrospin) or nmrPipe (*34*). Analysis of the spectral data was aided by CARA [R. Keller and K. Wuthrich, Computer-aided resonance assignment (CARA), available from http://www.nmr.ch] and AutoLink (*35*).

RESULTS

Expression of the CLR and RAMP1 ECDs. To facilitate biochemical and biophysical studies of the CGRP receptor and to provide a structural model for ligand binding, we sought to generate a soluble recombinant heterodimer comprising the first ECDs of human CLR and RAMP1. Efforts were focused on expression in *E. coli*, as this would allow isotopic labeling for NMR structural studies. The first 22 residues of CLR and the first 25 residues of RAMP1 encode signal peptides for membrane targeting (*36*) and were excluded from all constructs (Figure 2). An untagged, CLR construct corresponding to residues 23−133 (CLR_{23-133}) and an amino-terminal hexahistidine-tagged RAMP1 construct corresponding to residues 26−117 ($RAMP1_{26-117}$) yielded more than 20 mg of expressed protein per gram of cell paste and were present almost exclusively in the insoluble inclusion body fraction (Figure 3A). Inclusion bodies from both constructs could be effectively solubilized with 6 M guanidine hydrochloride and excess reducing agent and co-refolded to form a functional heterodimeric complex, as outlined in the following sections.

Refolding and Purification of a Soluble CLR_{23-133}−$RAMP1_{26-117}$ Complex. Like all family B GPCRs, the ECD of CLR contains six cysteine residues that are predicted to form three intramolecular disulfide bonds. The RAMP1 ECD is also predicted to contain three disulfide bonds. We first attempted to refold the expressed constructs individually in a refolding buffer containing a high concentration of arginine, in an attempt to limit aggregation. Refolding buffer also contained a reduced/oxidized glutathione shuffling system to promote correct disulfide bond formation. Successful refolding of CLR (*25*) and RAMP1 (*37*) ECDs has been achieved; however, a functional complex of the two ECDs had not been reported. While we were able to refold CLR_{23-133} to yield a product containing the correct number of disulfide bonds [as determined by mass spectrometry (data not shown)], our refolding attempt for $RAMP1_{26-117}$ resulted in low yields, which form heterogeneous soluble aggregates at concentrations of > 1 mg/mL (data not shown). Reasoning that CLR_{23-133} and $RAMP1_{26-117}$ might form a complex, we attempted to refold the two ECD constructs together. The co-refolding yielded a stable, monodisperse, heterodimeric complex as evidenced by the co-elution of CLR_{23-133} and $RAMP1_{26-117}$ ECDs throughout all steps of purification. The resolution of the co-refolded ECDs by anion-exchange chromatography resulted in two prominent peaks that were well separated over the linear ionic gradient. Mass spectrometry, N-terminal sequencing and SDS−PAGE analysis (Figure 3B) confirmed the presence of both CLR_{23-133} and $RAMP1_{26-117}$ in the first peak and only excess CLR_{23-133} in the second (mass spectrometry and sequencing data not shown). Fractions corresponding to the first peak were pooled, concentrated, and resolved by gel filtration chromatography. As shown in Figure 4A, a single symmetric peak was observed, as expected if the two ECDs formed a complex. This peak had a retention volume between those for 44 and 17 kDa molecular mass standards, in agreement with a predicted molecular mass of 23839 Da for the monodisperse CLR_{23-133}−$RAMP1_{26-117}$ complex. SDS−PAGE analysis from the gel filtration fractions revealed the comigration of CLR_{23-133} and $RAMP1_{26-117}$ (Figure 3C). The retention volume (15.2 mL) and shape of the peak for the CLR_{23-133}−$RAMP1_{26-117}$ heterodimer remained relatively unchanged over the protein concentration range of 0.5−20 mg/mL (data not shown). By comparison, isolated CLR_{23-133} (0.5 mg/mL; expected molecular mass of 13139 Da) resolved under identical conditions gave rise to a peak with a retention volume of 15.6 mL (Figure 4C). This indicates a smaller Stokes radius for the isolated CLR_{23-133} compared to the CLR_{23-133}−$RAMP1_{26-117}$ complex, as expected if the latter comigrated as a complex. However, at higher concentrations (≥5 mg/mL), isolated CLR_{23-133} gave rise to additional peaks (Figure 4B) with decreased retention volumes, indicating a

A

MEKKCTLYFLVLLPFFMILVTAELEESPEDSIQLGVTRNKIMTAQYECYQKIMQDPIQQ
AEGVYCNRTWDGWLCWNDVAAGTESMQLCPDYFQDFDPSEKVTKICDQDGNWFRHPASN
RTWTNYTQCNVNTHEKVKTALNLFYLTIIGHGLSIASLLISLGIFFYFKSLSCQRITLH
KNLFFSFVCNSVVTIIHLTAVANNQALVATNPVSCKVSQFIHLYLMGCNYFWMLCEGIY
LHTLIVVAVFAEKQHLMWYYFLGWGFPLIPACIHAIARSLYYNDNCWISSDTHLLYIIH
GPICAALLVNLFFLLNIVRVLITKLKVTHQAESNLYMKAVRATLILVPLLGIEFVLIPW
RPEGKIAEEVYDYIMHILMHFQGLLVSTIFCFFNGEVQAILRRNWNQYKIQFGNSFSNS
EALRSASYTVSTISDGPGYSHDCPSEHLNGKSIHDIENVLLKPENLYN

B

MARALCRLPRRGLWLLLAHHLFMTTACQEANYGALLRELCLTQFQVDMEAVGETLWCDW
GRTIRSYRELADCTWHMAEKLGCFWPNAEVDRFFLAVHGRYFRSCPISGRAVRDPPGSI
LYPFIVVPITVTLLVTALVVWQSKRTEGIV

FIGURE 2: Schematic presentation of the full-length primary sequence of human CLR (A) and RAMP1 (B). For both CLR and RAMP1, the cleavable signal peptide is underlined. The ECDs for (A) CLR and (B) RAMP1 are colored yellow. Highlighted in gray for both sequences are the transmembrane region and cytoplasmic sequences.

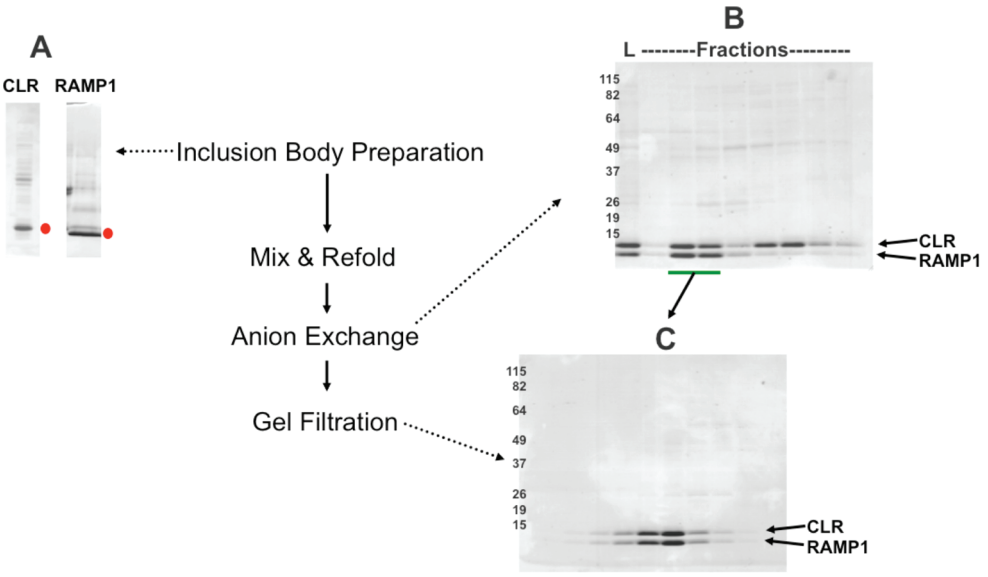

FIGURE 3: SDS−PAGE analysis from refolding and purification of inclusion bodies to generate a functional CLR_{23-133}−$RAMP_{126-117}$ complex for biophysical and structural studies. (A) Solubilization of inclusion bodies from the extracellular domains of CLR_{23-133} and $RAMP_{126-117}$ in 6 M guanidine hydrochloride in the presence of excess DTT. (B) Fractions from anion-exchange chromatography following refolding containing the co-eluted CLR_{23-133}−$RAMP_{126-117}$ complex (underlined). These fractions were pooled and applied on a gel filtration column. (C) Elutions from gel filtration showing comigration of CLR_{23-133} and $RAMP1_{26-117}$.

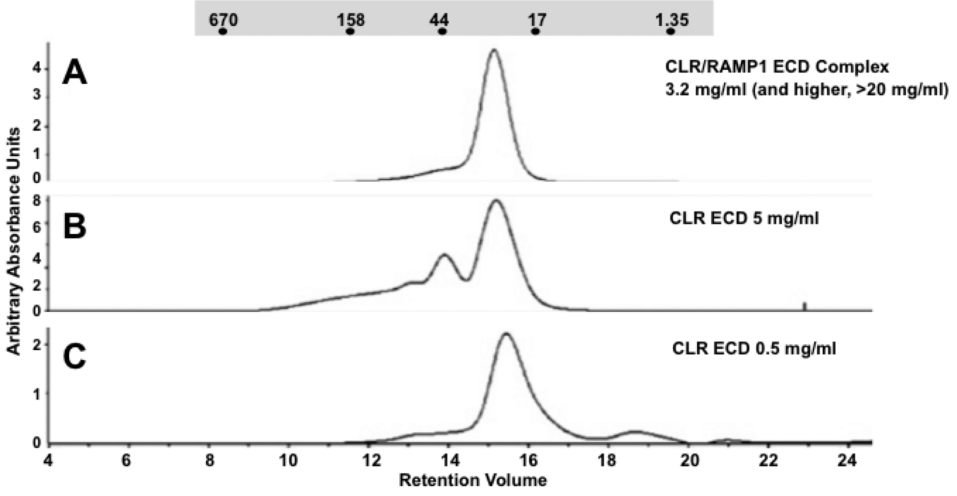

FIGURE 4: Comparison of S200 gel filtration chromatograms of the refolded CLR_{23-133}−$RAMP_{126-117}$ ECD complex at 3.2 mg/mL (A) with those for the refolded CLR_{23-133} ECD (in the absence of RAMP1) at 5 mg/mL (B) or 0.5 mg/mL (C), indicating the CLR_{23-133} ECD when refolded without $RAMP1_{26-117}$ forms higher-order aggregates at high concentrations. For the sake of simplification, arbitrary absorbance units (at 280 nm) are reported. The migration of molecular mass standards is shown (gray box).

Table 2: Sequences of hα-CGRP, Peptide Truncations, and Analogues[a]

peptide	sequence
hα-CGRP	ACDTATCVTHRLA-GLLSRSGGVVKNNF-VPTNVGSKAF-NH_2
11-mer$_{27-37}$ (D^{31}, P^{34}, F^{35})	FVPT**D**VG**PF**AF-NH_2
11-mer$_{27-37}$ (D^{31}, azaG^{33}, P^{34}, F^{35})	FVPT**D**Vaza**GPF**AF-NH_2
11-mer$_{27-37}$ (D^{31}, A^{34}, F^{35})	FVPT**D**VG**A**FAF-NH_2
8-mer$_{30-37}$ (D^{31}, P^{34}, F^{35})	T**D**VG**PF**AF-NH_2

[a]Residues shown in bold for shorter peptide sequences represent substitutions *versus* the native hα-CGRP sequence.

concentration-dependent aggregation and/or multimerization of this protein in the absence of $RAMP1_{26-117}$.

To identify the optimal pair of CLR and RAMP1 ECDs for X-ray crystallographic studies, a total of 16 combinations using four CLR and four RAMP1 constructs (Table 1) were refolded and purification of the soluble fraction monitored with the same procedures used for the CLR_{23-133}−$RAMP1_{26-117}$ complex described above. All construct pairs in Table 1 formed 1:1 complexes with elution profiles similar to that shown for the CLR_{23-133}−$RAMP1_{26-117}$ complex in Figure 4A; however, only the CLR_{23-133}−$RAMP1_{26-117}$ complex yielded diffracting crystals. As implied by the elution profiles, a 94-amino acid region of CLR (CLR_{40-133}) was sufficient for interaction with an 80-amino acid region of RAMP1 ($RAMP1_{26-105}$). Smaller N-terminal truncations of RAMP1 were not found in the soluble fraction after refolding and/or did not copurify with CLR.

Characterization of Ligand Binding to the CLR_{23-133}−$RAMP1_{26-117}$ ECD Complex. We then measured the ability of the purified CLR_{23-133}−$RAMP1_{26-117}$ complex to compete directly with [^{125}I]CGRP for binding to native CGRP receptors in SK-N-MC membranes. In this assay, the calculated IC_{50} for the CLR_{23-133}−$RAMP1_{26-117}$ complex was 12 ± 12 μM (Figure 5A).

We also developed a second, indirect, assay that would further permit us to measure the potency with which the CLR_{23-133}−$RAMP1_{26-117}$ complex could compete with wild-type CGRP receptors for binding to the CGRP peptide and olcegepant. In this experiment, binding of the CGRP peptide or olcegepant to the CLR_{23-133}−$RAMP1_{26-117}$ complex was expected to yield a concomitant increase in the level of [^{125}I]CGRP bound to the SK-N-MC membranes versus control reactions with BSA, but lacking the soluble ECD complex. This was because the CLR_{23-133}−$RAMP1_{26-117}$ complex would function as a "ligand sink", reducing the amount of unlabeled ligand available to compete with [^{125}I]CGRP binding to native receptors. As expected, both CGRP (IC_{50} = 233 ± 67 pM) and olcegepant (IC_{50} = 54 ± 25 pM) were able to compete with [^{125}I]CGRP binding to native CGRP receptors in the SK-N-MC membranes (Figure 5B). However, when the CGRP peptide was incubated with the CLR_{23-133}−$RAMP1_{26-117}$ complex, only slight shifts in the competition curves were generated (IC_{50} = 101 ± 21 pM) (Figure 5C), consistent with lower-affinity binding of CGRP to the soluble ECD complex. Addition of 1 μM CLR_{23-133}−$RAMP1_{26-117}$ complex to olcegepant titrations (10^{-12} to 10^{-6} M) almost completely eliminated the compound's ability to displace [^{125}I]CGRP from SK-N-MC membranes (Figure 5C). Moreover, the CLR_{23-133}−$RAMP1_{26-117}$ complex bound

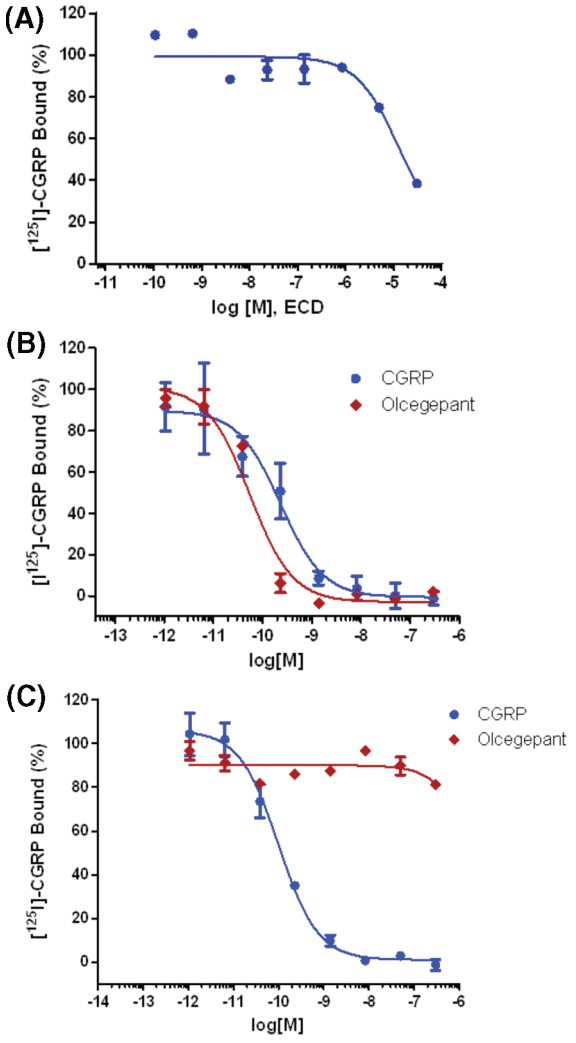

FIGURE 5: [^{125}I]CGRP radioligand binding studies. [^{125}I]CGRP binding to the native CGRP receptor in SK-N-MC membranes was assessed in the presence of increasing concentrations of (A) purified CLR_{23-133}−$RAMP1_{26-117}$ ECD complex and (B) unlabeled CGRP (blue circles) and olcegepant (red diamonds). (C) Indirect competition assay to measure the ability of the CLR_{23-133}−$RAMP1_{26-117}$ ECD complex to compete for binding to CGRP (blue circles) or olcegepant (red diamonds) in the presence of the native CGRP receptors in SK-N-MC membranes. In this experiment, increasing concentrations of CGRP or olcegepant were incubated with 1 μM CLR_{23-133}−$RAMP1_{26-117}$ complex followed by additions of SK-N-MC membranes containing the native receptors and [^{125}I]CGRP (see Experimental Procedures). All experiments producing data depicted in this figure were performed in triplicate.

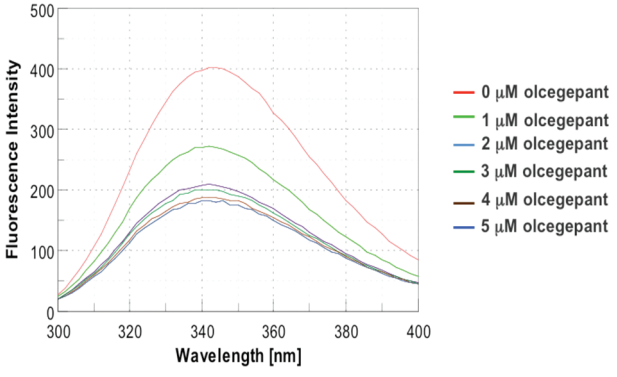

FIGURE 6: Stoichiometric quenching of the CLR_{23-133}−$RAMP_{126-117}$ ECD complex tryptophan fluorescence by titration with olcegepant.

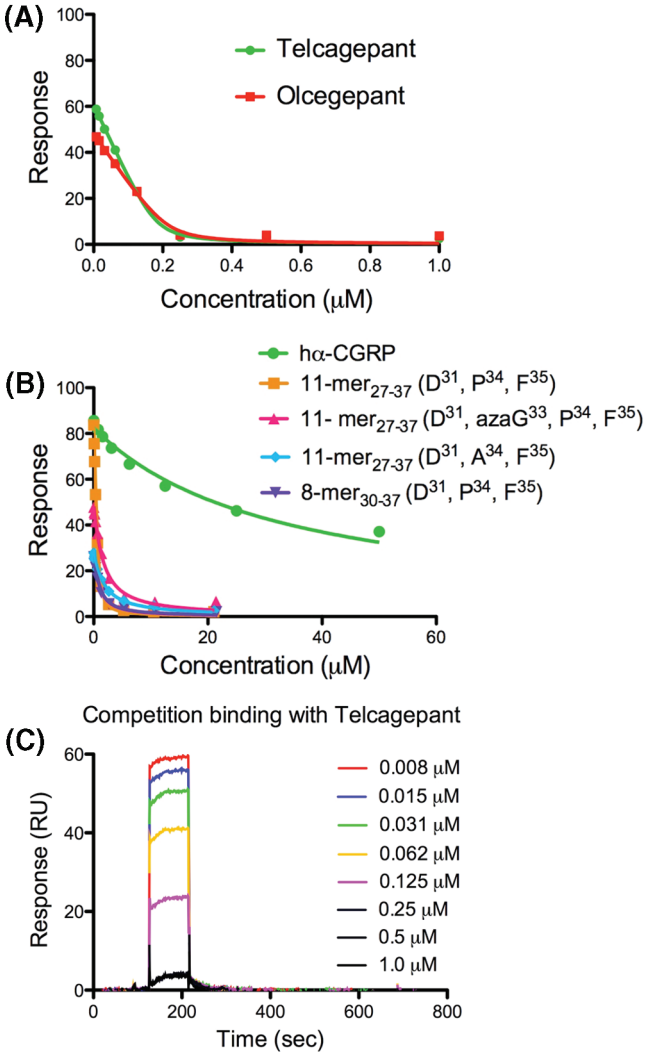

FIGURE 7: Steady state binding analysis of the refolded CLR_{23-133}–$RAMP_{26-117}$ ECD complex with telcagepant and olcegepant (A) and CGRP peptide variants (B) by SPR. Sensogram responses of the $CRLR_{23-133}$–$RAMP_{26-117}$ ECD complex to immobilized biotinylated CGRP at various concentrations of ligands. The dissociation constants were calculated from the binding isotherms by nonlinear regression analysis using PRISM version 5.0a. (C) Representative reference-corrected sensorgrams of the refolded CLR_{23-133}–$RAMP_{26-117}$ ECD complex preincubated with the indicated concentrations of telcagepant and monitored on a surface immobilized with biotinylated CGRP.

directly to olcegepant, as evidenced by a stoichiometric quenching of the ECD complex's intrinsic tryptophan fluorescence by olcegepant (Figure 6).

Surface Plasmon Resonance Competition Binding Studies. Having observed the weaker binding of the longer peptides and the more potent binding of olcegepant using the [^{125}I]CGRP competition binding methods, we sought to measure the affinities of the CLR_{23-133}–$RAMP1_{26-117}$ ECD complex directly using surface plasmon resonance methods. Shorter peptide analogues of $CGRP_{27-37}$ and $CGRP_{30-37}$ have been shown previously to bind with high nanomolar affinity to the full-length receptor (*15*, *38*). We tested these peptide analogues (Table 2) along with full-length CGRP, olcegepant, and telcagepant by assessing binding of the CLR_{23-133}–$RAMP1_{26-117}$ ECD complex to biotinylated CGRP in the presence of increasing concentrations of ligand. Under all tested conditions, a steady state plateau was reached within the first few seconds of injections (for example,

Table 3: SPR-Derived Equilibrium Binding Constants of Telcagepant, Olcegepant, and CGRP to the CLR_{23-133}–$RAMP1_{26-117}$ Ectodomain Complex

	K_D (μM) by SPR
hα-CGRP	23.6 ± 12.0
11-mer$_{27-37}$ (D^{31}, P^{34}, F^{35})	0.14 ± 0.02
11-mer$_{27-37}$ (D^{31}, $azaG^{33}$, P^{34}, F^{35})	1.16 ± 0.17
11-mer$_{27-37}$ (D^{31}, A^{34}, F^{35})	1.62 ± 0.24
8-mer$_{30-37}$ (D^{31}, P^{34}, F^{35})	0.56 ± 0.14
olcegepant	< 0.02
telcagepant	< 0.02

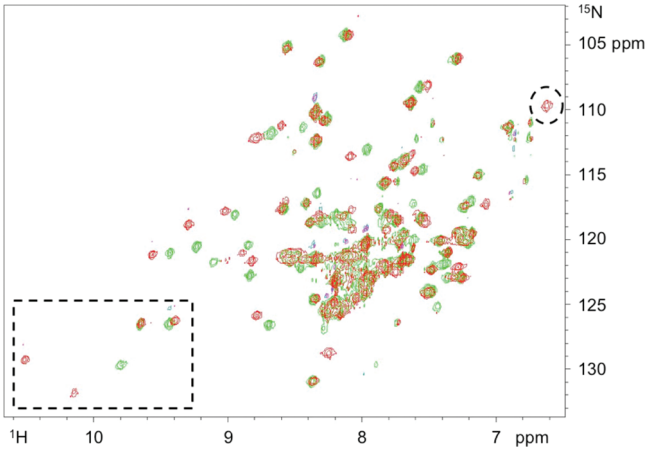

FIGURE 8: ^{15}N–^{1}H TROSY spectra of the unliganded unlabeled CLR_{23-133}–[^{15}N,^{13}C,^{2}H]$RAMP1_{26-117}$ complex (green peaks) and the olcegepant–unlabeled CLR_{23-133}–[^{15}N,^{13}C,^{2}H]$RAMP1_{26-117}$ ternary complex (red peaks). The oval denotes a new Thr amide resonance. The box shows the tryptophan indole NH region of the spectrum.

Figure 7C), making it possible to use the steady state R_{max} values to accurately calculate equilibrium constants for each ligand (Table 3 and Figure 7A,B). Full-length CGRP was determined to bind weakly to the CLR_{23-133}–$RAMP1_{26-117}$ ECD complex, with a K_D of 23.6 ± 12.0 μM, which is in the same affinity range as determined by the [^{125}I]CGRP binding assay (Figure 5A). Conversely, telcagepant and olcegepant both exhibited tight binding, each displaying a K_D value below the limit of detection for these measurements (K_D < 0.02 μM). In comparison to full-length CGRP, the shorter peptide analogues (Table 2) bound more tightly in the range of 140 nM to 1.62 μM (Table 3 and Figure 7).

NMR Structural Analysis of the CLR–RAMP1 ECD Complex. (*i*) *Antagonist-Induced Conformational Changes in* $RAMP1_{26-117}$. NMR methods can provide additional insight into the physicochemical properties, structure, and dynamics of proteins in solution. Chemical shift perturbation studies are particularly useful for identifying residues involved in and the conformational effects arising from ligand binding. Because of the heterodimeric nature of the CLR_{23-133}–$RAMP1_{26-117}$ ECD complex, a partial isotope labeling strategy was used to reduce spectral complexity: either the CLR ECD or the RAMP1 ECD was labeled with isotopes and refolded with the unlabeled counterpart. For CLR, a shorter construct lacking seven amino-terminal residues (CLR_{30-133}) had a higher level of expression in minimal medium (data not shown) and was used for all perdeuterated samples.

The ^{15}N–^{1}H TROSY spectrum of the unlabeled CLR_{23-133}–[^{15}N,^{13}C,^{2}H]$RAMP1_{26-117}$ complex is shown in Figure 8.

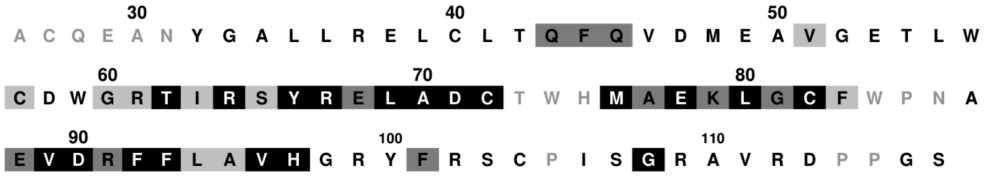

FIGURE 9: $RAMP1_{26-117}$ $^{15}N-^{1}H$ TROSY chemical shift perturbations observed upon addition of olcegepant to the ECD complex. Boxes containing residues are shaded according to the magnitude of the chemical shift perturbation observed upon ligand addition: no shading, no change from unliganded protein control; light gray shading, small shift [up to 0.04 ppm (^{1}H) and 0.3 ppm (^{15}N)]; medium gray shading, moderate shift [0.04−0.08 ppm (^{1}H) and 0.3−0.7 ppm (^{15}N)]; black shading, > 0.08 ppm (^{1}H) and > 0.7 ppm (^{15}N). Unassigned residues are denoted with gray text.

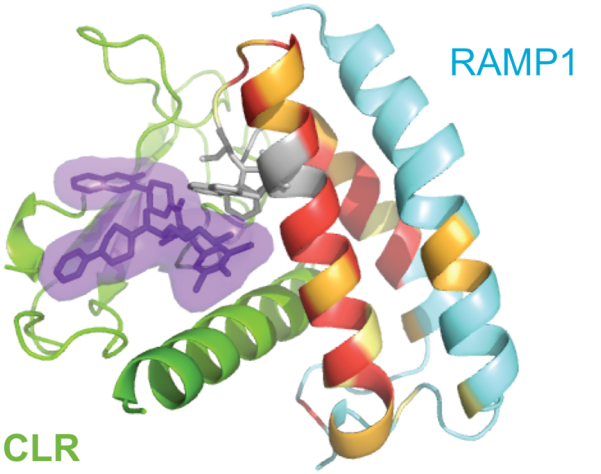

FIGURE 10: Perturbations observed by NMR when olcegepant (purple) binds to CLR_{23-133} (green) and $RAMP1_{26-117}$ (cyan). $RAMP1_{26-117}$ residues exhibiting amide chemical shift changes upon addition of ligand are colored according to small (yellow), moderate (orange), and large (red) magnitude effects. Unassigned gap residues are colored gray, and the side chains of W74 and W84 are shown. This figure was rendered using Pymol Molecular Graphics System (De Lano Scientific, Palo Alto, CA).

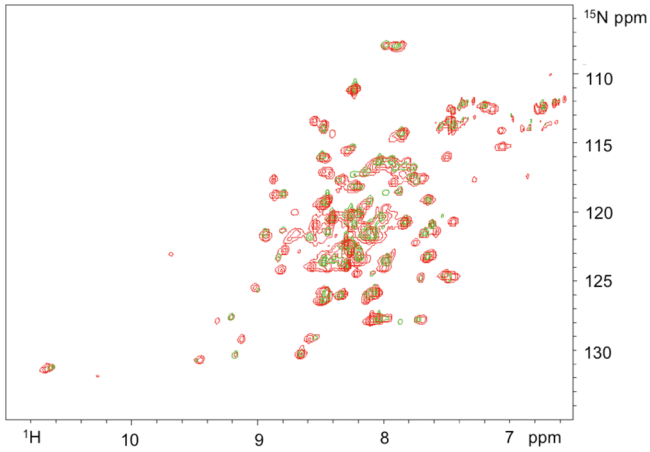

FIGURE 11: $^{15}N-^{1}H$ TROSY spectra of the unliganded [^{15}N,^{13}C]CLR_{23-133}−unlabeled RAMP complex (green peaks) and the olcegepant−[^{15}N,^{13}C]CLR_{23-133}−unlabeled RAMP ternary complex (red peaks).

Approximately 90% (78 of 87) of the backbone amide resonances of $RAMP1_{26-117}$ were assigned. The chemical shift dispersion and line widths are consistent with those of a folded, globular protein. Chemical shift indices and intrahelical amide−amide NOEs confirmed that the secondary structure of the protein was primarily α-helical. There are two gaps in the resonance assignments of $RAMP1_{26-117}$: the first occurs in the region near W74, a residue known to contribute to olcegepant binding (*39*, *40*), and the second at W84, located in the loop connecting helices αR2 and αR3 (*37*) (E. ter Haar et al., unpublished observations).

The effect of antagonist binding to $RAMP1_{26-117}$ was examined by measuring perturbations of amide chemical shifts in the $^{15}N-^{1}H$ TROSY spectrum induced by addition of olcegepant. Major changes to the spectrum occur upon addition of olcegepant, including the appearance of a new threonine spin system (oval, Figure 8), which can be assigned to T73 (the only remaining unassigned threonine residue). In the spectral region associated with tryptophan indole NH protons (unassigned), one new resonance appears and another shifts dramatically (box, Figure 8). Thus, it appears that residues in the T73-W74-H75 and W84-P85-N86 regions exhibit broad resonances due to backbone motions, but these motions are attenuated upon binding of olcegepant. Globally, olcegepant-induced chemical shift perturbations are observed for approximately half of the assigned amide resonances (Figure 9). The largest perturbations are clustered in the region from G60 to C82, which spans helix αR2 in the X-ray structures of RAMP1 (*37*) (E. ter Haar et al., unpublished observations). When the olcegepant-induced chemical shift perturbations are mapped onto the X-ray structure of the complex (Figure 10), it is found that 31 of the 39 affected amides are more than 10 Å from the ligand (including most of the shifted amides in helix αR2 and all of those in helices αR1 and αR3), indicating that the perturbations arise due to conformational changes rather than direct effects (such as ring current effects from aromatic rings on the ligand).

(*ii*) *$CLR_{23,30-133}$ Mobility and Conformational Heterogeneity in the Unliganded and Olcegepant-Bound States.* The $^{15}N-^{1}H$ TROSY spectrum of a complex of ^{15}N- and ^{13}C-labeled CLR_{23-133} and unlabeled $RAMP1_{26-117}$ is shown in Figure 11. The chemical shift dispersion and line widths are consistent with those of a folded, globular protein. However, multiple spectral features indicate that CLR_{23-133} contains even more regions of dynamic flexibility than $RAMP1_{26-117}$. For example, only 77 of 107 of the expected spin systems were observed in the $^{15}N-^{1}H$ TROSY and HNCO spectra for an unliganded sample, suggesting that a subset of residues in CLR_{23-133} have dynamic properties that broaden and obscure their NH resonances. In addition, the resonances that could be observed were of variable intensity and line width, a further indication that these resonances are undergoing broadening due to motions that are slow to intermediate on the NMR time scale.

Upon addition of olcegepant to the sample, significant changes were observed in the spectrum. These differences included shifts in a number of existing resonances as well as the appearance of numerous new resonances (Figure 11). In all, we identified

102 of 107 expected resonances in the $^{15}N-^{1}H$ TROSY spectrum. However, because of the absence of predicted correlations in the HNCACB and HN(CO)CACB spectra for a [^{13}C,^{15}N,^{1}H]-CLR_{23-133} labeled sample, we were not able to determine the sequential assignments. In an attempt to address these difficulties, data were collected for a sample of methyl-protonated {Ile(δ1 only),Leu($^{13}CH_3$,$^{12}CD_3$),Val($^{13}CH_3$,$^{12}CD_3$)} [^{15}N,^{13}C,^{2}H]-CLR_{30-133}−RAMP1 complex. Although we observe nearly all expected resonances in the $^{15}N-^{1}H$ TROSY spectrum (100 of 102), 90% of the expected C_α and C_α-1 correlations in the HNCA spectrum, and approximately 70% of the expected C_β and C_β-1 correlations in the HNCACB spectrum, unambiguous assignment of the spectra was still not possible. For example, there were three independent sets of amino acid NMR spin systems observed for which resonances could be assigned only to the unique CLR_{30-133} primary sequence element from Ser 98 to Thr 102. In addition, more methyl resonances in the $^{1}H-^{13}C$ correlation spectrum arising from leucine, isoleucine, and valine residues were detected than would be expected on the basis of the primary sequence and our labeling pattern (23 observed, 13 predicted) (data not shown). These results are consistent with the presence of multiple conformers in the sample that are stable or interconvert on a very slow NMR time scale.

DISCUSSION

The CGRP receptor is a heterodimer of CLR, a class B GPCR, and the accessory protein RAMP1. Small-molecule antagonists of the CGRP receptor have been shown to be efficacious for the treatment of migraine in the clinical setting (*6*, *7*). Unfortunately, like most GPCRs, structural studies of the CGRP receptor have been hampered by the lack of an abundant natural source for purification as well as the many difficulties that are inherent in the recombinant expression, solubilization, purification, and crystallization of membrane proteins. In this report, we have shown that the extracellular domains of CLR and RAMP1 can be expressed in milligram quantities in *E. coli* and then refolded to form a complex that is competent to bind known CGRP receptor antagonists. Further, we identified the subcomplex comprising residues 40−133 of CLR and residues 26−105 of RAMP1 as a minimal region of the receptor that forms a stable, monodisperse heterodimer. The ECD CLR_{23-133}−$RAMP1_{26-117}$ complex forms a stable heterodimer with 1:1 stoichiometry. Studies with the full-length receptor have shown that when CLR and RAMP1 are expressed together, the complex is targeted to the cell surface as a 1:1 heterodimer (*41*). In a later study using bioluminescence resonance energy transfer (BRET) methods (*42*), the same group reported that the CGRP receptor exists as a heterotrimer with 2:1 stoichiometry, i.e., a CLR homodimer associated with a RAMP1 monomer. While this latter study (*42*) suggests that functional heterotrimers do exist, it cannot rule out the possibility that most of receptors in the plasma membrane result from heterodimers of CLR and RAMP1. Our results for the extracellular domain complex of CLR and RAMP1 indicate a heterodimer with 1:1 stoichiometry, in agreement with the previous study of Hilaret et al. (*41*).

The ligand binding properties of the ECD CLR_{23-133}−$RAMP1_{26-117}$ complex were analyzed by several methods, and these revealed that the complex is a reasonable surrogate for small-molecule binding studies and structural analyses. Using the radioligand displacement binding assays, we first demonstrated that the ECD complex could compete directly with [^{125}I]CGRP for binding to native CGRP receptors, with an IC_{50} of 12 ± 12 μM. This IC_{50} value for the ECD complex was much higher than the subnanomolar affinity with which α-CGRP binds to high-affinity sites on native CGRP receptors reported here [233 ± 67 pM (Figure 5B)] and in the literature (*43*−*45*). However, additional competition binding studies designed to indirectly monitor the potency of binding of the ECD CLR_{23-133}−$RAMP1_{26-117}$ complex to ligands revealed that although the ECD complex has a lower affinity for CGRP than native CGRP receptors, high-affinity binding to small-molecule antagonists was preserved (Figure 5C). In these experiments, the ECD complex effectively acted as a sink for olcegepant, binding the small molecule with a significantly higher affinity than full-length CGRP. The affinities of several ligands were then directly measured in vitro using surface plasmon resonance. These studies confirmed high-affinity (K_D < 0.02 μM) binding of the CLR_{23-133}−$RAMP1_{26-117}$ complex to the small-molecule antagonists olcegepant and telcagepant, but comparatively weak binding to full-length CGRP (K_D = 23.6 ± 12.0 μM). Affinities of C-terminal peptide variants were also measured (Table 3), and these peptide antagonists bound the ECD complex with a much higher affinity than the full-length CGRP peptide. The weakest of these [11-mer$_{27-37}$ (D^{31}, P^{34}, F^{35})] (K_D = 1.62 μM) bound with ~15-fold higher affinity, while the 11-mer$_{27-37}$ (D^{31}, P^{34}, F^{35}) (K_D = 0.14 μM) bound with ~170-fold higher affinity than full-length CGRP. These results are most consistent with a model in which the ECD CLR_{23-133}−$RAMP1_{26-117}$ complex largely maintains the full-length receptor binding site(s) for small-molecule ligands (i.e., antagonists) but additional regions of the CGRP receptor, such as those contained in the juxtamembrane domain, likely contribute significantly to binding of full-length CGRP and related peptides. This is consistent with the two-domain binding model of class B GPCR activation (*46*), as well as with studies on other isolated class B GPCR ECDs, which likewise have lower affinities for endogenous peptide ligands than the full-length receptors (*46*−*48*).

For several reasons, the overall view of the ECD CLR−RAMP1 complex described by our NMR studies is that of a flexible, mobile receptor that undergoes significant changes in both conformation and dynamics upon ligand binding. In the case of $RAMP1_{26-117}$, binding of olcegepant perturbed approximately half of the amide resonances. The largest effects were observed throughout helix αR2 and its C-terminal loop, as well as the residues it contacts on helices αR1 and αR3. This pattern suggests that helix αR2 moves significantly upon ligand binding. Furthermore, new RAMP1 resonances appeared for the olcegepant-liganded complex. The most plausible explanation is that these correspond to T73, W74, and W84 (resonances unassigned in the unliganded complex). Thus, ligand binding likely slows backbone motions in this region. This hypothesis is consistent with previous mutagenesis studies implicating W74 of RAMP1 in conferring species selectivity for small-molecule antagonists (*40*, *49*, *50*), as well as the X-ray structure of the complex of the ECD with olcegepant (Figure 10) (E. ter Haar et al., unpublished observations), which shows that the ligand contacts the indole rings of both W74 and W84. The NMR results for CLR_{30-133} also showed that the addition of antagonist yields significant spectral changes. Moreover, it is clear from our analysis that, in solution, the CLR subunit does not have a single defined tertiary, and perhaps in some regions, secondary structure. Conformational heterogeneity in the free state is an intrinsic property of GPCRs in general (*51*, *52*). The observed

conformational heterogeneity in the unliganded state for both CLR and RAMP1 is not surprising for a GPCR ectodomain that must bind ligand and transduce a signal through the membrane. Even in the liganded state, conformational heterogeneity for CLR is still observed, but motions that resulted in the broadening or disappearance of amide resonances in the unliganded state are attenuated when olcegepant is bound. Similar dynamic effects were observed with the homologous protein corticotropin releasing factor type 2 (CRFR2) (*53*). CRFR2 contains two loops that appear disordered in the unliganded state. Upon addition of the antagonist peptide astressin, loop 2, near the peptide binding site, becomes more ordered, while loop 1, distal from the peptide binding site, remains flexible. It appears that similar effects occur for CLR in the unliganded and antagonist-bound states.

To summarize, we have taken a reductionist approach to express and purify a stable, functional extracellular domain of the CGRP receptor. Comprising a heterodimer of the extracellular domains of CLR and RAMP1, this complex was competent to bind both peptide and small-molecule antagonists and suitable for structural analyses by NMR. Using this production strategy, we have also recently obtained the X-ray crystal structure of the CGRP receptor ectodomain in the unliganded state and in complex with several small-molecule antagonists (E. ter Haar et al., unpublished observations). Since no full-length class B GPCR−RAMP complex has yet been produced at levels sufficient for structural studies, this complex serves as a valuable, structurally accessible surrogate for the design of new CGRP receptor-targeted migraine therapeutics.

ACKNOWLEDGMENT

We thank K. Bonnano and D. Briggs for assistance with cell growth and inclusion body preparations. We thank G. Iyer and S. Pazhanisamy for assistance with collection and analysis of SPR data.

REFERENCES

1. Brain, S. D., Williams, T. J., Tippins, J. R., Morris, H. R., and MacIntyre, I. (1985) Calcitonin gene-related peptide is a potent vasodilator. *Nature 313*, 54–56.
2. Doods, H., Arndt, K., Rudolf, K., and Just, S. (2007) CGRP antagonists: Unravelling the role of CGRP in migraine. *Trends Pharmacol. Sci. 28*, 580–587.
3. Link, A. S., Kuris, A., and Edvinsson, L. (2008) Treatment of migraine attacks based on the interaction with the trigeminocerebrovascular system. *J. Headache Pain 9*, 5–12.
4. Goadsby, P. J., Edvinsson, L., and Ekman, R. (1990) Vasoactive peptide release in the extracerebral circulation of humans during migraine headache. *Ann. Neurol. 28*, 183–187.
5. Lassen, L. H., Haderslev, P. A., Jacobsen, V. B., Iversen, H. K., Sperling, B., and Olesen, J. (2002) CGRP may play a causative role in migraine. *Cephalalgia 22*, 54–61.
6. Olesen, J., Diener, H. C., Husstedt, I. W., Goadsby, P. J., Hall, D., Meier, U., Pollentier, S., and Lesko, L. M. (2004) Calcitonin gene-related peptide receptor antagonist BIBN 4096 BS for the acute treatment of migraine. *N. Engl. J. Med. 350*, 1104–1110.
7. Ho, T. W., Ferrari, M. D., Dodick, D. W., Galet, V., Kost, J., Fan, X., Leibensperger, H., Froman, S., Assaid, C., Lines, C., Koppen, H., and Winner, P. K. (2008) Efficacy and tolerability of MK-0974 (telcagepant), a new oral antagonist of calcitonin gene-related peptide receptor, compared with zolmitriptan for acute migraine: A randomised, placebo-controlled, parallel-treatment trial. *Lancet 372*, 2115–2123.
8. McLatchie, L. M., Fraser, N. J., Main, M. J., Wise, A., Brown, J., Thompson, N., Solari, R., Lee, M. G., and Foord, S. M. (1998) RAMPs regulate the transport and ligand specificity of the calcitonin-receptor-like receptor. *Nature 393*, 333–339.
9. Fluhmann, B., Muff, R., Hunziker, W., Fischer, J. A., and Born, W. (1995) A human orphan calcitonin receptor-like structure. *Biochem. Biophys. Res. Commun. 206*, 341–347.
10. Born, W., Fischer, J. A., and Muff, R. (2002) Receptors for calcitonin gene-related peptide, adrenomedullin, and amylin: The contributions of novel receptor-activity-modifying proteins. *Receptors Channels 8*, 201–209.
11. Chakder, S., and Rattan, S. (1990) [Tyr0]-calcitonin gene-related peptide 28−37 (rat) as a putative antagonist of calcitonin gene-related peptide responses on opossum internal anal sphincter smooth muscle. *J. Pharmacol. Exp. Ther. 253*, 200–206.
12. Chiba, T., Yamaguchi, A., Yamatani, T., Nakamura, A., Morishita, T., Inui, T., Fukase, M., Noda, T., and Fujita, T. (1989) Calcitonin gene-related peptide receptor antagonist human CGRP-(8−37). *Am. J. Physiol. 256*, E331–E335.
13. Maggi, C. A., Chiba, T., and Giuliani, S. (1991) Human α-calcitonin gene-related peptide-(8−37) as an antagonist of exogenous and endogenous calcitonin gene-related peptide. *Eur. J. Pharmacol. 192*, 85–88.
14. Rovero, P., Giuliani, S., and Maggi, C. A. (1992) CGRP antagonist activity of short C-terminal fragments of human alpha CGRP, CGRP(23−37) and CGRP(19−37). *Peptides 13*, 1025–1027.
15. Carpenter, K. A., Schmidt, R., von Mentzer, B., Haglund, U., Roberts, E., and Walpole, C. (2001) Turn structures in CGRP C-terminal analogues promote stable arrangements of key residue side chains. *Biochemistry 40*, 8317–8325.
16. Rist, B., Entzeroth, M., and Beck-Sickinger, A. G. (1998) From micromolar to nanomolar affinity: A systematic approach to identify the binding site of CGRP at the human calcitonin gene-related peptide 1 receptor. *J. Med. Chem. 41*, 117–123.
17. Doods, H., Hallermayer, G., Wu, D., Entzeroth, M., Rudolf, K., Engel, W., and Eberlein, W. (2000) Pharmacological profile of BIBN4096BS, the first selective small molecule CGRP antagonist. *Br. J. Pharmacol. 129*, 420–423.
18. Iovino, M., Feifel, U., Yong, C. L., Wolters, J. M., and Wallenstein, G. (2004) Safety, tolerability and pharmacokinetics of BIBN 4096 BS, the first selective small molecule calcitonin gene-related peptide receptor antagonist, following single intravenous administration in healthy volunteers. *Cephalalgia 24*, 645–656.
19. Ittner, L. M., Koller, D., Muff, R., Fischer, J. A., and Born, W. (2005) The N-terminal extracellular domain 23−60 of the calcitonin receptor-like receptor in chimeras with the parathyroid hormone receptor mediates association with receptor activity-modifying protein 1. *Biochemistry 44*, 5749–5754.
20. Fitzsimmons, T. J., Zhao, X., and Wank, S. A. (2003) The extracellular domain of receptor activity-modifying protein 1 is sufficient for calcitonin receptor-like receptor function. *J. Biol. Chem. 278*, 14313–14320.
21. Kuwasako, K., Kitamura, K., Nagoshi, Y., Cao, Y. N., and Eto, T. (2003) Identification of the human receptor activity-modifying protein 1 domains responsible for agonist binding specificity. *J. Biol. Chem. 278*, 22623–22630.
22. Hilairet, S., Foord, S. M., Marshall, F. H., and Bouvier, M. (2001) Protein-protein interaction and not glycosylation determines the binding selectivity of heterodimers between the calcitonin receptor-like receptor and the receptor activity-modifying proteins. *J. Biol. Chem. 276*, 29575–29581.
23. Koller, D., Born, W., Leuthauser, K., Fluhmann, B., McKinney, R. A., Fischer, J. A., and Muff, R. (2002) The extreme N-terminus of the calcitonin-like receptor contributes to the selective interaction with adrenomedullin or calcitonin gene-related peptide. *FEBS Lett. 531*, 464–468.
24. Salvatore, C. A., Mallee, J. J., Bell, I. M., Zartman, C. B., Williams, T. M., Koblan, K. S., and Kane, S. A. (2006) Identification and pharmacological characterization of domains involved in binding of CGRP receptor antagonists to the calcitonin-like receptor. *Biochemistry 45*, 1881–1887.
25. Chauhan, M., Rajarathnam, K., and Yallampalli, C. (2005) Role of the N-terminal domain of the calcitonin receptor-like receptor in ligand binding. *Biochemistry 44*, 782–789.
26. Grauschopf, U., Lilie, H., Honold, K., Wozny, M., Reusch, D., Esswein, A., Schafer, W., Rucknagel, K. P., and Rudolph, R. (2000) The N-terminal fragment of human parathyroid hormone receptor 1 constitutes a hormone binding domain and reveals a distinct disulfide pattern. *Biochemistry 39*, 8878–8887.
27. Sprangers, R., Velyvis, A., and Kay, L. E. (2007) Solution NMR of supramolecular complexes: Providing new insights into function. *Nat. Methods 4*, 697–703.
28. Paone, D. V., Shaw, A. W., Nguyen, D. N., Burgey, C. S., Deng, J. Z., Kane, S. A., Koblan, K. S., Salvatore, C. A., Mosser, S. D.,

Johnston, V. K., Wong, B. K., Miller-Stein, C. M., Hershey, J. C., Graham,
S. L., Vacca, J. P., and Williams, T. M. (2007) Potent, orally bioavailable calcitonin gene-related peptide receptor antagonists for the treatment of migraine: Discovery of N-[(3R,6S)-6-(2,3-difluorophenyl)-2-oxo-1-(2,2,2-trifluoroethyl)azepan-3-yl]-4-(2-oxo-2,3-dihydro-1H-imidazo-[4,5-b]pyridin- 1-yl)piperidine-1-carboxamide (MK-0974). *J. Med. Chem. 50*, 5564–5567.

29. Rudolf, K., Eberlein, W., Engel, W., Pieper, H., Entzeroth, M., Hallermayer, G., and Doods, H. (2005) Development of human calcitonin gene-related peptide (CGRP) receptor antagonists. 1. Potent and selective small molecule CGRP antagonists. 1-[N2-[3, 5-dibromo-N-[[4-(3,4-dihydro-2(1H)-oxoquinazolin-3-yl)-1-piperidinyl]carbonyl]-D-tyrosyl]-l-lysyl]-4-(4-pyridinyl)piperazine: The first CGRP antagonist for clinical trials in acute migraine. *J. Med. Chem. 48*, 5921–5931.
30. Zimmermann, U., Fischer, J. A., and Muff, R. (1995) Adrenomedullin and calcitonin gene-related peptide interact with the same receptor in cultured human neuroblastoma SK-N-MC cells. *Peptides 16*, 421–424.
31. Loria, J. P., Rance, M., and Palmer, A. G., III (1999) Transverse-relaxation-optimized (TROSY) gradient-enhanced triple-resonance NMR spectroscopy. *J. Magn. Reson. 141*, 180–184.
32. Salzmann, M., Pervushin, K., Wider, G., Senn, H., and Wuthrich, K. (1998) TROSY in triple-resonance experiments: New perspectives for sequential NMR assignment of large proteins. *Proc. Natl. Acad. Sci. U.S.A. 95*, 13585–13590.
33. Salzmann, M., Wider, G., Pervushin, K., and Wuthrich, K. (1999) Improved sensitivity and coherence selection for [^{15}N,^{1}H]-TROSY elements in triple resonance experiments. *J. Biomol. NMR 15*, 181–184.
34. Delaglio, F., Grzesiek, S., Vuister, G. W., Zhu, G., Pfeifer, J., and Bax, A. (1995) NMRPipe: A multidimensional spectral processing system based on UNIX pipes. *J. Biomol. NMR 6*, 277–293.
35. Masse, J. E., and Keller, R. (2005) AutoLink: Automated sequential resonance assignment of biopolymers from NMR data by relative-hypothesis-prioritization-based simulated logic. *J. Magn. Reson. 174*, 133–151.
36. Nielsen, H., Engelbrecht, J., Brunak, S., and von Heijne, G. (1997) Identification of prokaryotic and eukaryotic signal peptides and prediction of their cleavage sites. *Protein Eng. 10*, 1–6.
37. Kusano, S., Kukimoto-Niino, M., Akasaka, R., Toyama, M., Terada, T., Shirouzu, M., Shindo, T., and Yokoyama, S. (2008) Crystal structure of the human receptor activity-modifying protein 1 extracellular domain. *Protein Sci. 17*, 1907–1914.
38. Boeglin, D., Hamdan, F. F., Melendez, R. E., Cluzeau, J., Laperriere, A., Heroux, M., Bouvier, M., and Lubell, W. D. (2007) Calcitonin gene-related peptide analogues with aza and indolizidinone amino acid residues reveal conformational requirements for antagonist activity at the human calcitonin gene-related peptide 1 receptor. *J. Med. Chem. 50*, 1401–1408.
39. Hay, D. L., Christopoulos, G., Christopoulos, A., and Sexton, P. M. (2006) Determinants of 1-piperidinecarboxamide, N-[2-[[5-amino-l-[[4-(4-pyridinyl)-l-piperazinyl]carbonyl]pentyl]amino]-1- [(3,5-dibromo-4-hydroxyphenyl)methyl]-2-oxoethyl]-4-(1,4-dihydro-2-oxo-3(2 H)-quinazolinyl) (BIBN4096BS) affinity for calcitonin gene-related peptide and amylin receptors: The role of receptor activity modifying protein 1. *Mol. Pharmacol. 70*, 1984–1991.
40. Mallee, J. J., Salvatore, C. A., LeBourdelles, B., Oliver, K. R., Longmore, J., Koblan, K. S., and Kane, S. A. (2002) Receptor activity-modifying protein 1 determines the species selectivity of non-peptide CGRP receptor antagonists. *J. Biol. Chem. 277*, 14294–14298.
41. Hilairet, S., Belanger, C., Bertrand, J., Laperriere, A., Foord, S. M., and Bouvier, M. (2001) Agonist-promoted internalization of a ternary complex between calcitonin receptor-like receptor, receptor activity-modifying protein 1 (RAMP1), and β-arrestin. *J. Biol. Chem. 276*, 42182–42190.
42. Heroux, M., Breton, B., Hogue, M., and Bouvier, M. (2007) Assembly and signaling of CRLR and RAMP1 complexes assessed by BRET. *Biochemistry 46*, 7022–7033.
43. Moore, E. L., Burgey, C. S., Paone, D. V., Shaw, A. W., Tang, Y. S., Kane, S. A., and Salvatore, C. A. (2009) Examining the binding properties of MK-0974: A CGRP receptor antagonist for the acute treatment of migraine. *Eur. J. Pharmacol. 602*, 250–254.
44. Poyner, D. R., Sexton, P. M., Marshall, I., Smith, D. M., Quirion, R., Born, W., Muff, R., Fischer, J. A., and Foord, S. M. (2002) International Union of Pharmacology. XXXII. The mammalian calcitonin gene-related peptides, adrenomedullin, amylin, and calcitonin receptors. *Pharmacol. Rev. 54*, 233–246.
45. Schindler, M., and Doods, H. N. (2002) Binding properties of the novel, non-peptide CGRP receptor antagonist radioligand, [^{3}H]BIBN4096BS. *Eur. J. Pharmacol. 442*, 187–193.
46. Hoare, S. R. (2005) Mechanisms of peptide and nonpeptide ligand binding to Class B G-protein-coupled receptors. *Drug Discovery Today 10*, 417–427.
47. Lopez de Maturana, R., Willshaw, A., Kuntzsch, A., Rudolph, R., and Donnelly, D. (2003) The isolated N-terminal domain of the glucagon-like peptide-1 (GLP-1) receptor binds exendin peptides with much higher affinity than GLP-1. *J. Biol. Chem. 278*, 10195–10200.
48. Perrin, M. H., DiGruccio, M. R., Koerber, S. C., Rivier, J. E., Kunitake, K. S., Bain, D. L., Fischer, W. H., and Vale, W. W. (2003) A soluble form of the first extracellular domain of mouse type 2β corticotropin-releasing factor receptor reveals differential ligand specificity. *J. Biol. Chem. 278*, 15595–15600.
49. Barwell, J., Miller, P. S., Donnelly, D., and Poyner, D. R. (2010) Mapping interaction sites within the N-terminus of the calcitonin gene-related peptide receptor; the role of residues 23−60 of the calcitonin receptor-like receptor. *Peptides 31*, 170–176.
50. Miller, P. S., Barwell, J., Poyner, D. R., Wigglesworth, M. J., Garland, S. L., and Donnelly, D. (2010) Non-peptidic antagonists of the CGRP receptor, BIBN4096BS and MK-0974, interact with the calcitonin receptor-like receptor via methionine-42 and RAMP1 via tryptophan-74. *Biochem. Biophys. Res. Commun. 391*, 437–442.
51. Kobilka, B. K., and Deupi, X. (2007) Conformational complexity of G-protein-coupled receptors. *Trends Pharmacol. Sci. 28*, 397–406.
52. Tao, Y. X. (2008) Constitutive activation of G protein-coupled receptors and diseases: Insights into mechanisms of activation and therapeutics. *Pharmacol. Ther. 120*, 129–148.
53. Grace, C. R., Perrin, M. H., Gulyas, J., Digruccio, M. R., Cantle, J. P., Rivier, J. E., Vale, W. W., and Riek, R. (2007) Structure of the N-terminal domain of a type B1 G protein-coupled receptor in complex with a peptide ligand. *Proc. Natl. Acad. Sci. U.S.A. 104*, 4858–4863.